



ELSEVIER

Surface Science 397 (1998) 225–236

surface science

Modeling the interaction of hydrogen with silicon surfaces

Daniela Kohen, John C. Tully¹, Frank H. Stillinger**Lucent Technologies, Bell Laboratories Innovations, 700 Mountain Avenue, Murray Hill, NJ 07974, USA*

Received 6 June 1997, accepted for publication 15 September 1997

Abstract

We have investigated the prospects for developing model potentials for use in classical simulation of structural and dynamical properties of Si surfaces interacting with hydrogen. The point of view adopted requires that only short-range two-atom and three-atom interactions appear, and that these component functions should be fully transferable between small-molecule gas phase species (e.g. SiH and H₂) and Si surfaces with arbitrary extent of hydrogenation. Using the silicon Stillinger–Weber potential as a starting point and guide, a moderately successful set of such interaction functions was derived by non-linear parameter optimization. This set displays proper bonding geometries and valence saturation when applied to several hydride species of intermediate molecular weight (e.g. Si₄H₁₀ and Si₁₀H₁₆), and to dimerized Si(100) in various stages of hydrogenation. Molecular dynamics simulations show relatively large sticking probabilities for impinging H atoms at low incident energies, whereas H₂ at comparable energies experiences only non-sticking collisions, both roughly in agreement with experiment. Some shortcomings of the derived model have been identified, including deficient surface diffusion kinetics, however, possible improvement strategies have been identified. © 1998 Published by Elsevier Science B.V.

Keywords: Ab initio quantum chemical methods and calculations, Catalysis, Chemisorption, Density functional calculations, Hydrogen, Molecular dynamics simulations, Semiconducting surfaces, Silicon

1. Introduction

Silicon plays a central role in modern computing and communications technology, so it is natural that vast experimental and theoretical resources have been devoted to understanding its properties (for a detailed review see Ref. [1]). As device applications move inexorably to shorter and shorter length scales, interface and surface characteristics gain in relative importance. In particular, it is desirable to explore and analyze the nature of

chemical bonding at the surface of crystalline silicon, including both kinetic aspects and static structures.

The present paper concerns the development of computer simulation models for the chemical interactions of hydrogen with crystalline silicon. The specific objectives are to determine the feasibility of representing the admittedly complicated atomic interactions by a relatively simple mathematical format (just two- and three-atom interactions), and to test that simple format in a classical molecular dynamics simulation routine.

Prior experience lends support to this approach. The two-atom plus three-atom approximation has attained modest success for pure silicon itself [2], as well as germanium [3], both strongly covalent

* Corresponding author. Fax (+1) 908 5823958, e-mail dohen@lucent.com

¹ Current address: Chemistry Department, Yale University, New Haven, CT 06511, USA

substances. Surface reaction of fluorine with silicon also yields to this approach [4,5]. Therefore, encouraging evidence has been gathered on the success of this approach in conveying valency and bond directionality of the various elements involved.

In fact, Carter and coworkers [6] have even examined the modeling of crystalline silicon hydrogenation by the two-atom plus three-atom approximation; however, their emphasis and tactics differ from ours, as explained below. In addition, Murty and Atwater [7] have proposed an alternative representation for Si plus H potentials, but this alternative is not confined to two- and three-body contributions.

In the following, Section 2 presents and motivates the mathematical format employed. It also states the data base of molecular properties used to determine numerical parameters appearing in the mathematical format, the procedure used for their determination, and the two-atom and three-atom interactions thus obtained. Section 3 describes several structural properties that were investigated. Section 4 contains a description of our molecular dynamics simulation procedure, as well as several results obtained from its use. Finally, Section 5 presents a discussion of several issues related to our approach, and draws some conclusions about its extension and possible improvement.

2. Model

The molecular dynamics simulation process to be described below presumes to follow motions of atoms moving on their Born–Oppenheimer ground-state potential energy surface Φ . Our first task is to create a physically and chemically sensible approximation for Φ that is applicable to arbitrary configurations of arbitrary numbers of silicon and hydrogen atoms. We have assumed that Φ can be adequately represented by a linear combination of two-atom and three-atom functions, for all pairs and triplets present:

$$\Phi = \sum v_{\text{SiSi}} + \sum v_{\text{HH}} + \sum v_{\text{SiH}} + \sum v_{\text{SiSiSi}}^{(3)} + \sum v_{\text{HHH}}^{(3)} + \sum v_{\text{SiSiH}}^{(3)} + \sum v_{\text{SiHH}}^{(3)}. \quad (1)$$

Each of the component functions appearing here must possess translational, rotational, and permutational symmetries; in particular this forces the pair potentials to depend only on scalar pair distances.

In order to simplify the present task, we have adopted at the outset the Stillinger and Weber functions v_{SiSi} and $v_{\text{SiSiSi}}^{(3)}$ for the pure silicon part of our problem [2]. The first of these has the following generic form:

$$v_{\text{SiSi}}(r) = \begin{cases} \alpha(\beta r^{-p} - 1) \exp[\gamma/(r-a)] & \text{if } r < a, \\ 0 & \text{if } r \geq a, \end{cases} \quad (2)$$

where all five constants, α , β , p , γ , and a are positive. This pair interaction expresses the tendency for covalent bond formation, but by itself cannot control bonding directionality or valence saturation. These latter attributes are enforced through the three-atom interaction, which for convenience has been resolved into three components:

$$v_{\text{SiSiSi}}^{(3)} = h(r_{i,j}, r_{i,k}, \theta_{j,l,k}) + h(r_{j,l}, r_{j,k}, \theta_{l,j,k}) + h(r_{k,j}, r_{k,l}, \theta_{j,k,l}). \quad (3)$$

Here the $r_{i,j}$ are scalar pair distances in the triad and $\theta_{i,j,k}$ is the vertex angle at j subtended by l and k . The Stillinger–Weber model assigns to h the functional form [2]

$$h(r_{i,j}, r_{i,k}, \theta_{j,l,k}) = \begin{cases} \lambda [\cos(\theta_{j,k,l}) + \frac{1}{3}]^2 \exp[\gamma^{(3)}/r_{i,j} - a^{(3)}] & \text{if } r < a^{(3)}, \\ 0 & \text{otherwise.} \end{cases} \quad (4)$$

The three constants λ , $\gamma^{(3)}$, and $a^{(3)}$ are positive. The use of finite-distance cut-offs in the pure silicon interaction functions, along with the use of a format that preserves continuity and differentiability of all orders at those cut-offs, was motivated by computational simplicity and efficiency. This becomes particularly important in many-atom simulations. It is a strategy we have maintained in the present extension to include hydrogen.

Five functions in Eq. (1) remain to be determined. Known properties of several small molecules provide a basis for selection. These include:

(a) the diatomics H₂ and SiH [8]; (b) H₂+H, specifically the geometry and energy of the transition state [9,10], (c) geometries and energies of silicon hydrides SiH₂, SiH₃, SiH₄, and Si₂H₆ (references below). Although it is impossible to fit all attributes simultaneously and exactly, we have attempted to identify the best overall fit under the functional constraints adopted.

Our first step was to fix $v_{\text{HH}}(r)$ and $v_{\text{SiH}}(r)$ using known diatomic bond lengths, dissociation constants, and normal-mode vibrational frequencies [8]. The same generic functional form as shown in Eq. (2) for $v_{\text{SiSi}}(r)$ was used, but with the possibility of distinct numerical parameters. Note that if for each pair of atoms the cut-off a and the exponent of the atom pair distance p are first chosen, the other parameters can be calculated analytically to reproduce the known properties of the diatomics detailed in (a) above; this was used in the selection procedure

The final parameter set selected appears in Table 1. Fig. 1 shows plots of the three pair potentials.

The equilibrium bond length for SiH, 1.52 Å, is close to the corresponding bond lengths in the polyatomic silicon hydrides in (c) above. Consequently, the task of the remaining three-atom functions is to enforce bond angles and valence saturation in these species. We have supposed that the following generalizations of Eqs (3) and (4) were applicable ($i, j, k = \text{Si, H}$):

$$v_{i,j,k}^{(3)} = h_{i,j,k}(r_{i,j}, r_{j,k}, \theta_{i,j,k}) + h_{j,i,k}(r_{j,i}, r_{i,k}, \theta_{j,i,k}) + h_{i,k,j}(r_{i,k}, r_{k,j}, \theta_{i,k,j}) \quad (5)$$

where, following earlier convention, the middle

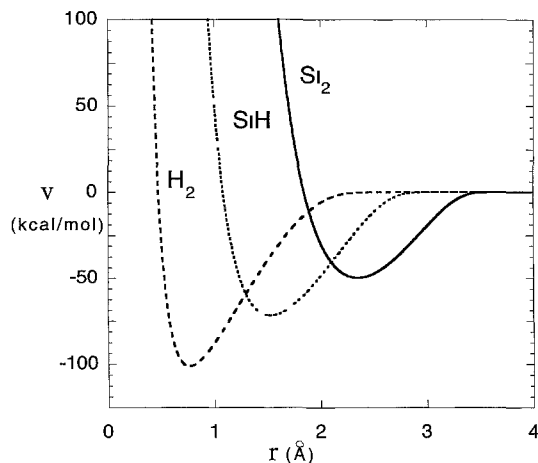


Fig. 1 Si-Si, H-H, and Si-H pair potentials vs distance

letter of the triad subscript refers to the species at the subtended angle vertex. The individual component functions have been extended slightly in form to

$$h_{i,j,k}(r_{i,j}, r_{j,k}, \theta_{i,j,k}) = \begin{cases} \lambda_{i,j,k} [1 + \mu_{i,j,k} \cos(\theta_{i,j,k}) + v_{i,j,k} \cos(\theta_{i,j,k})^2] \\ \exp[\gamma_{i,j,k}^{(3)}/(r_{i,j} - a_{i,j,k})] & \text{if } r_{i,j} < a_{i,j,k}^{(3)} \text{ and} \\ + \gamma_{(i),j,k}/(r_{j,k} - a_{(i),j,k}) & r_{j,k} < a_{(i),j,k}^{(3)}, \\ 0 & \text{otherwise,} \end{cases} \quad (6)$$

where the atom in parentheses in $\gamma_{i,k,(j)}$ is the third atom in the triad, the one that does not participate in the “leg” under consideration. Notice that unequal parameters are permitted along the distinct “legs” of a species-asymmetric triad. This change allows a different rate of decay of the radial part for each “leg” and was introduced as a response to the fact that in certain molecules the difference in atom bonding distances is quite important, e.g. Si-H (1.49 Å) vs Si-Si (2.33 Å) in disilane.

Note that h is separable into an angular and a radial component of the interaction. This is the third constraint in the form of the potential being adopted, the first being the restriction to three- and two-body interactions and the second being

Table 1
Two-body interaction potential parameters. Units are kcal mol⁻¹ and Å

Atoms	$v_{xy}(r) = \alpha_{xy}(\beta_{xy} r^{-p} - 1) \exp\left[\frac{\gamma_{xy}}{(r - a_{xy})}\right]$ if $r < a_{xy}$				
	α	β	γ	a	p
Si Si	352 477814	11 603192	2 095100	3 771180	4
H H	804 959233	0 044067	3 902767	2 8	4
Si H	428 902380	1 359978	2 537884	3 2	4

the short range of the potential introduced by the cut-offs.

The three-body function $v_{\text{HHH}}^{(3)}$ was first independently fixed, using the data (b) above. This is a symmetrical triad case for which all h -function “legs” are identical. Table 2 shows the numerical values that were assigned to the parameters. Subsequently, the SiH_2 , SiH_3 , and SiH_4 data allowed simultaneous optimization of h_{SiHH} and h_{HSiH} (the first has the single Si at the end of a leg, the second at the vertex common to the two legs), with parameter values also reported in Table 2. This fixes all but h_{SiSiH} and h_{SiHSi} , so, the final stage involves the properties of disilane, Si_2H_6 , to complete the task. Again, results appear in Table 2. The remaining free parameters in these stages were subjected to non-linear optimization; however, the results were not unique due to “ruggedness” of the parameter hypersurface. Consequently, the collection of optima was examined individually to identify which was chemically the most valid; see Table 2.

Table 3 shows bond distances, angles, and energies for the four silicon hydride molecules employed as input. Entries contain both the experimental input data and the results obtained by potential energy minimization for our model after its functions were all determined. Agreement, as expected, is not perfect but is sufficiently close to encourage further use of the model.

3. Structural properties

Beyond simply providing an adequate fit to the molecular input data, the model must demonstrate

its ability to produce reasonable predictions in new and different situations. Consequently, several elementary tests were devised to assure the model's chemical validity, at least at a coarse level of description. We regard successful performance in these tests as a necessary prerequisite for molecular dynamics simulation of surface properties. Moreover, we have found some sets of parameters, and subsequently discarded them, that fit the input data as well as the ones shown in Tables 1 and 2 but perform poorly when subjected to the tests described below.

Two types of test were performed: searches for minimum-energy structures and dynamical simulations. In the rest of this section the structural studies will be described; note that among these we include all those that render some information about structural properties even when the technique used to locate potential energy minima was that of a simulation. The dynamical studies, both the tests and the simulations that were used only as a means to characterize the model, will be described in Section 4 as will the methodology behind the simulations.

The minimum-energy structure for a set of four hydrogen atoms should consist of two intact H_2 molecules, weakly interacting with each other. Indeed this is the result of the energy minimization for the model constructed. Evidently, valence saturation is assured for the model potential, at least for pure hydrogen.

Several cases with an arbitrary number of silicon and hydrogen atoms in both arbitrary as well as plausible initial configurations were studied. They

Table 2
Three-body interaction potential parameters. Units are kcal mol^{-1} and \AA .

$$h(j,k,l) = \lambda_{jlk} [1 + \mu_{jlk} \cos(\theta_{jlk}) + \nu_{jlk} \cos(\theta_{jlk})^2] \exp \left[\frac{\gamma_{lj}(k)}{(r_{lj} - \chi_{jlk})} + \frac{\gamma_{lk}(l)}{(r_{lk} - \chi_{jlk})} \right]$$

$j-k$	λ	μ	ν	$\gamma_{lj}(k)$	$\gamma_{lk}(l)$	χ
Si-Si-Si	166 666667	6 000000	9 000000	2 514120	2 514120	3 771180
H-H-H	403 005000	0 132587	-0 299700	1 500000	1 500000	2 80
H-Si-H	100 633157	7 200000	10 800000	2 212406	2 212406	3 20
Si-H-H	557 667194	-2 939390	1 800000	0 558821	3 328492	3 20
Si-Si-H	17 110500	12 000000	18 000000	1 848715	2 539432	3 40
Si-H-Si	2000 000	-0 400000	-0 600000	2 400000	2 400000	3 40

Table 3
Molecular parameters from experiment and from the model

Molecule	Energy (kcal mol ⁻¹)		Bond length (Å)		Symmetry		Angle (deg)	
	Exp	This work	Exp	This work	Exp	This work	Exp	This work
SiH ₄	302.8 ^a	302.50	1.48 ^d	1.470	<i>T_d</i>	<i>T_d</i>	109.47	109.47
SiH ₃	214.0 ^b	222.73	1.48	1.471	<i>C_{3v}</i>	<i>C_{3v}</i>	111.2 ^e	106.31
SiH ₂	144.4 ^c	145.06	1.48	1.474	<i>C_{2v}</i>	<i>C_{2v}</i>	92.4 ^e	102.61
Si ₂ H ₆	500.1 ^{f,g}	500.10						
Si–Si			2.331 ^d	2.325				
Si–H			1.492 ^d	1.470				
Si–Si–H							110.3 ^d	112.2
H–Si–H							108.6 ^d	106.6

^a Based on enthalpy of formation given in Ref [11]

^b Based on enthalpy of formation given in Ref. [12]

^c Based on enthalpy of formation given in Ref [13]

^d Ref [14]

^e Ref [15].

^f Ref [16]

^g Ref [17]

confirmed that the model being described here sustains a tetravalent Si and a monovalent H. The lowest energy structure was always the one expected.

Two large molecules were specifically investigated, Si₄H₁₀ and Si₁₀H₁₆, since they are suitable intermediates between small molecules (which were being used as input) and a macroscopic surface (which is a primary goal of study). The result of the minimizations, i.e. the equilibrium structures in this model, are shown in Fig. 2; these structures are qualitatively close to the ones previously calculated by other authors using quantum chemistry techniques [15].

The model also accurately reproduces the structure of a Si(100) 2 × 1 surface that remains dimerized but is otherwise fully hydrogenated (see Fig. 3). The Si–Si–H angle is 112°, only slightly higher than the reported 108–111° [18]. The binding energy of one H, 72.6 kcal mol⁻¹, is in the range of reported binding energies, 61.5 kcal mol⁻¹ (an indirect measurement [19]) and 89.9 kcal mol⁻¹ (ab initio calculation for a small cluster [20] and that of the H₃Si–H bond in silane [21]).

The partially hydrogenated (100) surface is not

as well described by the model. A known characteristic of this surface is that it is energetically favorable for two H atoms to be bonded to the two silicon atoms of the same surface silicon dimer rather than to silicon atoms of different dimers. This observation has been attributed to the fact that a dimer π-bond needs to be broken when an H binds to the surface [22]. The model described here does not reproduce this phenomenon, and given the short range of the interactions there is no thermodynamic preference for the relative position of two hydrogen atoms on the surface.

One of the obvious attributes expected of any model of the type considered is that the insertion of an H atom into the interior of a perfect Si crystal should be energetically costly. We have verified that our specific model possesses this characteristic. In particular, we find a mechanically stable structure, lying 101 kcal mol⁻¹ above the energy of the H bonded to the surface. Its configuration is that of a hydrogen atom symmetrically bridging two silicon atoms with an Si–H distance of 1.55 Å, with corresponding distortion in the slab. Coincidentally, its energy agrees exactly with result of an ab initio quantum mechanical calculation by Van de Walle [23].

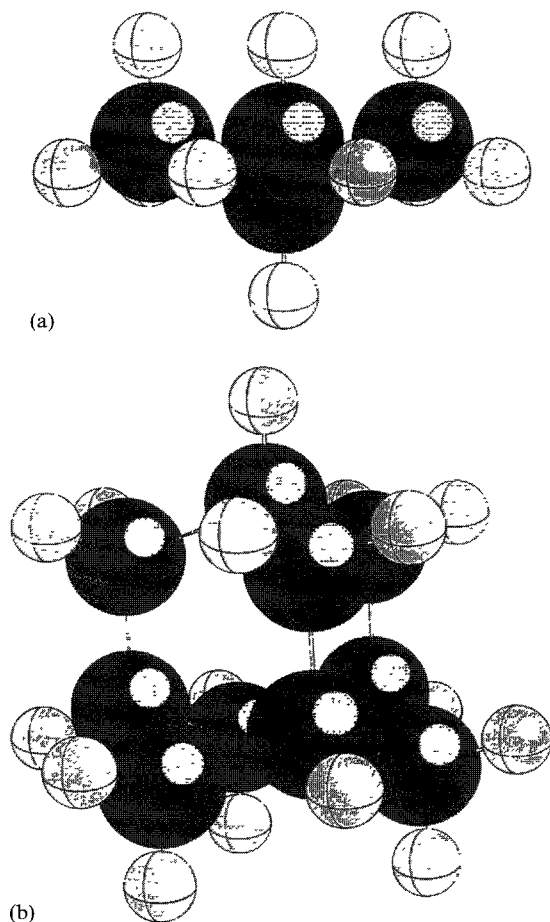


Fig 2 Si_4H_{10} and $\text{Si}_{10}\text{H}_{16}$ equilibrium structures predicted by this model. The Si atoms are dark and the H atoms are light. The molecules are shown to scale. In the first molecule all the Si–Si distances are 2.33 Å, the Si–H distances are 1.47 Å when the Si is attached to three H atoms, and 1.52 Å when attached to only one H atom. All the Si–Si–Si angles are 109.4°, the H–Si–H angles are 106.7°, the Si–Si–H angles are 112.2° when the H shares the Si with other H atoms and 109.6° when it does not. In the second molecule all the Si–Si distances are 2.34 Å, the Si–H distances are 1.47 Å when the Si is attached to two H atoms and 1.52 Å when attached to only one H atom. All the Si–Si–Si angles are 109.8°, the H–Si–H angles are 102.8°, the Si–Si–H angles are 111.4° when the H shares the Si with another H atom and 109.6° when it does not.

4. Molecular dynamics simulation

It was mentioned earlier that we have performed several molecular dynamics simulations studying an Si(100) 2×1 surface interacting with hydrogen.

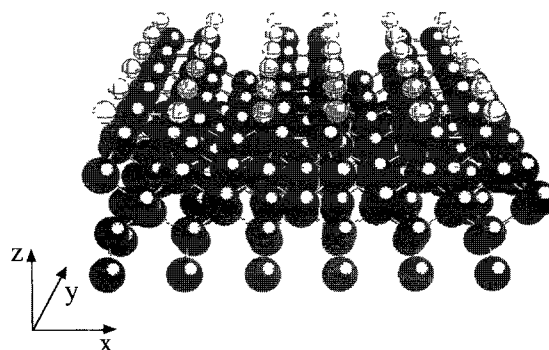


Fig 3 Structure of the fully hydrogenated Si(100) 2×1 surface predicted by this model. The size of the slab is the same as that for which the molecular dynamics studies were performed. The Si–H distances are 1.52 Å, and the Si–Si–H angles are 112°.

In this section we present the methodology used and the results obtained.

Unless specifically noted, all simulations employed an initial configuration of 216 silicon atoms in a primary cell of $23.0252 \text{ \AA} \times 23.0252 \text{ \AA} \times \text{infinity}$ with periodic boundary conditions in the short directions x and y . The crystalline silicon slab at the center of this infinite column consisted of six layers of 36 atoms each. The slab was crystallographically oriented to expose (100) faces at the top and bottom of the slab, i.e. normal to the z -direction. The lowest silicon layer was rigidly fixed at bulk crystal positions throughout the simulations. All other atoms execute undamped classical motion subject to the potential energy function described above. The minimum energy configuration of the top layer is a reconstructed $p(2 \times 1)$ pattern composed of 18 silicon dimers of bond length 2.42 Å.

The total energy is conserved throughout the simulation. Initial positions and momenta were selected in the following way. Positions were chosen such that all the silicon atoms were located at their minimum energy sites. Momenta were chosen at random from a Boltzmann distribution at twice the desired temperature. Classical equations of motion for the system of movable atoms (the 180 Si plus the necessary H atoms) were integrated using the velocity Verlet algorithm [24]. The time step length and length of the runs depended on the particular applications, but in all

cases it was checked that the final result converged with respect to these parameters.

The structural results described in Section 3, that is the structure of the fully hydrogenated surface, the respective energies of two H atoms in different positions on the surface, and the structure of an H atom embedded in the slab were obtained by simulated annealing. This was performed by first giving the system some energy (300 K) and letting it evolve for 1 ps. After this preparation period it continued evolving, but every so often all the atom velocities were scaled downward by 0.99 until the total kinetic energy was negligible. The static configuration thus obtained is what was reported earlier. This procedure was repeated for many initial states to ensure that the global minimum energy configuration was determined.

In the case of a hydrogen atom embedded in the slab, the z direction (previously infinite in extent) was given periodic boundary conditions corresponding to eight layers. Hence the primary cell adopts dimensions $23.0252 \text{ \AA} \times 23.0252 \text{ \AA} \times 9.504 \text{ \AA}$. This simulation was started at 0 K and the initial position of the H was slightly displaced from the geometric midpoint in a cavity. The final configuration was described in Section 3. The stability of this metastable minimum was investigated by relaxing the boundary condition in the z direction and letting the slab evolve at 300 K; under this circumstance the H remained firmly bonded to its bridge site.

A molecular dynamics simulation used as a test is that of the sticking probability of an H atom impinging on the Si(100) 2×1 surface at low temperature. The goal was to obtain a model potential that did not inadvertently produce unphysical surface-H atom interactions for configurations far from the equilibrium one. The related, secondary goal was to obtain a model potential that closely reproduced the near unity sticking probability measured experimentally [25]. In the unit mesh on the surface, see Fig. 4, a point grid was established. At the beginning of each trajectory an H atom was located in one of those grid points at a distance from the surface large enough to ensure that there were no interactions between the H and the surface. In all the runs reported in detail here, the slab was initially at

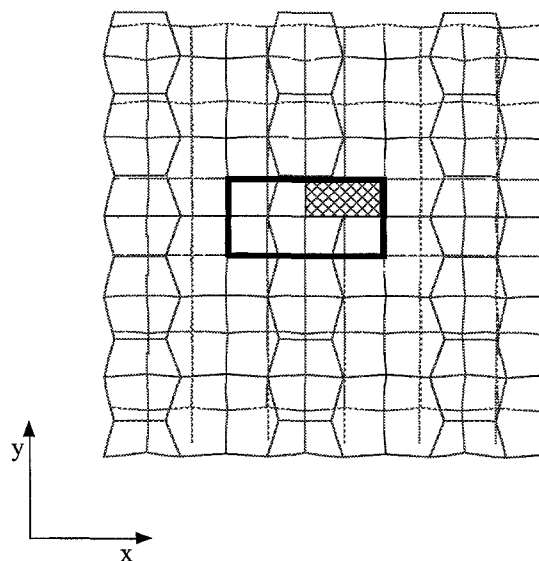


Fig. 4. Top view of the Si(100) 2×1 surface (wire frame). The point grid (see text) was established within the shaded region. The area surrounding a dimer, enclosed by the rectangle, is the one shown in Figs. 5–7.

0 K and the H approached the surface with normal incidence. Runs with different angles of approach were also examined but they did not provide significant additional information. In all cases the runs were long enough that the H either escaped from the field of interaction with the surface or was firmly bound to the surface. Three different sets of 116 runs were considered; they differed from each other by the initial velocity of the H. Fig. 5 shows the results of these runs. In Fig. 5a the initial velocity corresponds to a kinetic energy of 2 kcal mol^{-1} , Fig. 5b 1 kcal mol^{-1} and Fig. 5c $0.2 \text{ kcal mol}^{-1}$. In these cases the sticking probability is 78%, 86% and 78% respectively, and though they are not as high as reported experimentally (virtually unity), they were high enough to give credibility to the model.

The different initial conditions help in understanding which features of the potential give rise to the scattering (non-sticking) of the H in some trajectories. For 2 kcal mol^{-1} incident energy we notice that most of the scattered trajectories are located in a triangular region to the outside of the dimer (see Figs. 5 and 6) and that this region appears smaller in the 1 kcal mol^{-1} case and yet

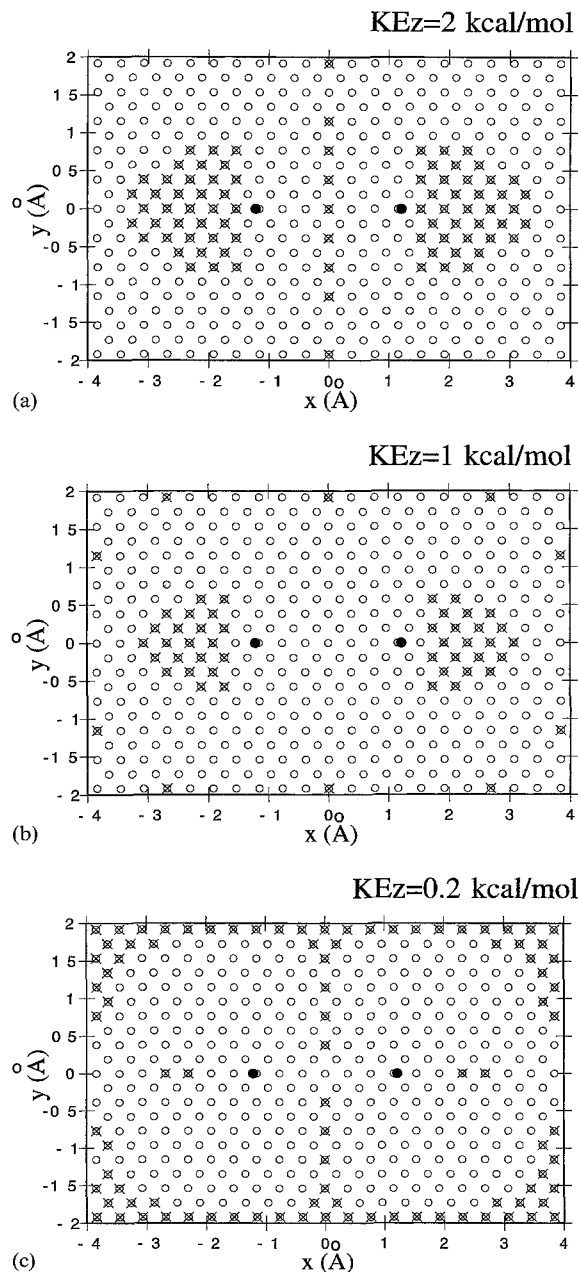


Fig. 5 Results of the normal incidence H sticking probability studies. The open circles indicate the position where each H was located at $t=0$. The closed circles indicate the position of each Si in the silicon dimer. The crosses indicate the initial position of the H atoms that scattered from the surface, i.e. did not stick. Total incident kinetic energy (in the z direction). (a) $2.0 \text{ kcal mol}^{-1}$, (b) $1.0 \text{ kcal mol}^{-1}$, and (c) $0.2 \text{ kcal mol}^{-1}$.

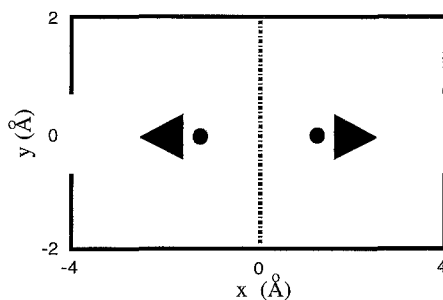


Fig. 6 Schematic figure showing the regions associated with the different behaviors exhibited when an H atom impinges onto the Si(100) surface. Solid circles represent the position of the two Si atoms of a dimer. The triangles and lines are described in the text.

even smaller in the $0.2 \text{ kcal mol}^{-1}$ case. This suggests that energy transfer is inefficient in this region and that the H atoms that impinge upon the surface do indeed get close to the surface; however, during the interaction time they do not lose enough kinetic energy to allow them to remain bound. Thus, this effect is purely kinetic; even though in this region the H atoms experience the largest attractive force to the slab, the transfer of energy is not fast enough to guarantee a sticking event.

This may well represent qualitatively correct dynamics. Another feature of the model that appears in these runs is the behavior in the perimeter around a complete dimer (see Fig. 5 and the solid line region in Fig. 6). In this region the model potential exhibits a small energy barrier between the binding site and the vacuum. This explanation is supported by the fact that the higher the incident energy is, then the more likely it is that the H binds to the surface when incident in this region. The presence of this energy barrier almost certainly represents an error in the model potential. Moreover, note how in the absence of this thin region, the sticking probabilities increase to 88%, 88% and 84% respectively. The last feature is another region of low-energy-transfer-rate, that of the line between the dimerized atoms, perpendicular to their bond (see Fig. 5 and the broken line in Fig. 6). This is reflected by the fact that at 2 kcal mol^{-1} the H atoms scatter from the surface and at 1 kcal mol^{-1} they bind to it. The behavior of atoms approaching this line with

0.2 kcal mol⁻¹ of kinetic energy is that of atoms that cannot overcome a barrier and, therefore, scatter; this indicates the presence of a small (less than 1 kcal mol⁻¹) barrier to binding. All the above characterizations are supported by the examination of the actual trajectories (not shown).

The battery of tests described above was used to select the final set of parameters for the model potential, as listed in Table 2. Once these parameters were finalized, additional molecular dynamics simulations were carried out, as described below.

The first of these studies is hydrogen migration on the Si(100) 2×1 surface. Even though the diffusion barriers have not been measured experimentally they have been calculated [6,26,27] and are crucial in the understanding hydrogen molecule desorption [28,29]. This is a very important problem owing to its relevance to the semiconductor industry as a potential rate-limiting step in several chemical vapor deposition processes. To perform this study the same grid sampling of the unit mesh as in the sticking probability study was used (see Fig. 5). A different simulated annealing run was performed with an H atom in each of these locations. The *x* and *y* position of the H were not allowed to change, but all the other coordinates, including those of the silicon slab, were. Thus, the minimum energy configuration of the slab plus a hydrogen atom subjected to the constraints just described was determined. All the runs began with the H far enough away to avoid any interaction with the surface and with some kinetic energy in the direction of the surface; if the H moved too far from the surface its momentum was reversed. The simulated annealing was performed in the manner described for the case of a fully hydrogenated surface.

The results are shown in Fig. 7. The figure presents a binding energy contour diagram. Note the anisotropic landscape. This agrees qualitatively with other authors' calculations, but the magnitude of the barriers are different in detail from those previously calculated by more accurate methods. In our model the possible diffusion pathways are between two Si atoms in the same dimer with a barrier of 39.7 kcal mol⁻¹ and in the same dimer row with a barrier 40.26 kcal mol⁻¹. The previous value reported for the diffusion barrier between

sites in a dimer is <36.4 kcal mol⁻¹ [6] (in the work being referenced the barriers were calculated along a straight line path and therefore may constitute upper bounds to the true barrier value) and for the diffusion along dimer rows is 32 kcal mol⁻¹ [27] and <38 kcal mol⁻¹ [6]. The results for the last possible diffusion path, between rows of dimers, are not in such a good agreement: the reported value is 44 kcal mol⁻¹ [27] and <62.8 kcal mol⁻¹ [6] but in our potential the only way that an H can diffuse between rows of dimers is if it first dissociates from the surface, with a barrier of 72.58 kcal mol⁻¹, the binding energy of an H to its equilibrium position. Even though this difference is in the highest barrier value, and therefore in the least employed path of diffusion, it still points to a flaw in the model potential.

Another study that was performed is that of the frequencies of the different normal modes of a hydrogenated surface. The H–Si–Si–H symmetric and antisymmetric stretch modes at a dimer were calculated and compared with experimental data [30,31]. To do so, the H atoms were displaced from their equilibrium positions in such a way that the normal mode whose frequency was going to be calculated was predominately excited and a representative property was recorded. For example, when the H–Si–Si–H symmetric stretch was calculated both the H–Si bonds were symmetrically stretched in the direction of the bond and the sum of the H–Si distances recorded as a function of time. The system was allowed to evolve for long enough that the recorded information was sufficient to permit a Fourier transform that gave detailed frequency information. The reported frequencies of the symmetric and antisymmetric stretch are 2098 cm⁻¹ and 2088 cm⁻¹, respectively. When the frequencies were calculated using our model potential the splitting was not reproduced, in both cases the frequencies were 2049.9 cm⁻¹. Comparing those with the frequency of the diatomic SiH, 2041.8 cm⁻¹ we note that the ones calculated using this model are shifted in the right direction, but not enough. These results, although not particularly bad, also point to the rigidity of the model presented here.

Finally, the qualitative behavior of a hydrogen molecule impinging in the surface was investigated. The reactivity of molecular hydrogen towards the

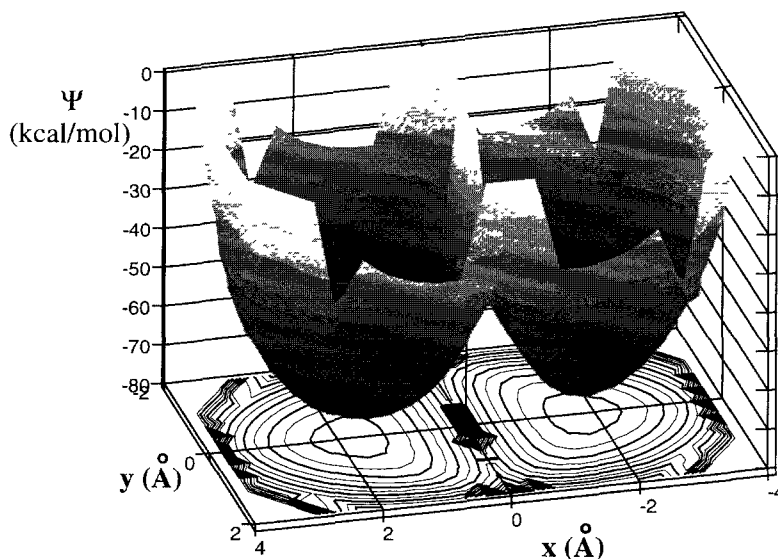


Fig. 7. Equal energy contours of the binding energy of an H atom to the Si(100) surface as a function of lateral x, y position. The z position and the Si atom coordinates were relaxed to minimize the total binding energy. The gray scale reflects the binding energy values.

silicon surface is known to be very low [32,33]. Using our model potential this result was reproduced. A total of 54 runs was performed. In all of them the temperature of the slab was 300 K, and the initial distance between H atoms was 1.1 times the equilibrium one; in half of them the kinetic energy of the incident H_2 molecule was $0.04 \text{ kcal mol}^{-1}$ (half in each H atom), and in the other half the kinetic energy of the incident H_2 molecule was $4.00 \text{ kcal mol}^{-1}$. Also, in all cases the hydrogen molecule approached the surface with the internuclear axis parallel to the surface, but the orientation of that axis with respect to the silicon dimers varied: in each set there were nine parallel, nine perpendicular and nine at 45° . Given the qualitative nature of this run, a detailed description of the dynamics observed is not pertinent here. The fact that not one of the molecules stuck to the surface, either intact or dissociatively, is the crucial one, and represents qualitative agreement with the experimental data.

5. Discussion and conclusions

The model presented in this paper has several virtues, but also a major weakness: the resultant

interaction between the silicon surface and an H atom is too rigid in the angular portion; the tetrahedral angle is preferred to an exaggerated extent. This is a reflection of a lack of a fully satisfactory compromise between two competing requirements. On the one hand the angular part in the H–Si–H three-body term needs to have a minimum in the angle that discriminates strongly in favor of pairs of bonds emanating from the vertex with the correct geometry, so that no more atoms than the ones that the valence dictates will bind preferentially. Note that this effect should be rather strong; the bond energy of H–H ($103.266 \text{ kcal mol}^{-1}$) is much larger than for Si–H ($70.5636 \text{ kcal mol}^{-1}$) so that if, for example, no three body-terms were used to construct “ SiH_4 ” all the H atoms would collapse close to each other (see Fig. 8). On the other hand, the experimentally measured virtually unity sticking probability and



Fig. 8. Stable “ SiH_4 ” that results using this potential without the three body terms.

the ease of diffusion of H on the silicon surface implies that there should be some binding at any angle. Unfortunately, in the model presented here the attraction to the surface occurs in most but not all angles, causing both the sticking probability to be lower than unity and the “unphysical” barrier to the diffusion of hydrogen on the surface to be too high.

A related model that does not exhibit this shortcoming is that of Carter and coworkers [6]. The goal of their work was to examine rates of diffusion of a single H adatom on an Si(100) 2×1 surface. Although they used functional forms for the interactions of Si–Si–H that are quite similar to ours, the parameters were fitted only to the results of first-principles electronic-structure calculation of H adatom adsorption and diffusion on embedded silicon clusters. They developed a model with good agreement between empirical and *ab initio* results and, therefore, had confidence that the potential thus obtained had predictive abilities in the regime that concerned them. The fact that their and our goals differ causes some shortcomings of that model from our viewpoint (it does not reproduce the SiH bond energy and the interactions of an Si atom with two or more H atoms were not modeled).

Several changes in the form of the potential and in the search procedure described above were investigated. All the changes were restricted by the constraints described earlier: three- and two-body interactions, short range of the potential introduced by the cut-offs, and separability between angular and radial parts in the form of the interactions. These attempted changes were: (a) the use of the normal mode frequencies of SiH₄ [15] as input in the fitting procedure; (b) higher order terms in the cosine expansion in the angular functional form; (c) the use of a different cut-off for each of the legs in the *h* function. These alternatives did not produce any improvement of the fitted potential, and since they complicated the fitting procedure they were ultimately not used.

The changes that are apparently necessary are very different in form than those just described. A change that will probably result in a higher sticking probability and a reduction of unphysical barriers to diffusion is that of longer-range interactions.

This could be achieved by a number of methods, for example by adding a long-range van der Waals interaction to pair interaction terms only. The addition of such terms would result in a numerically more costly model, but their inclusion seems necessary. Clearly, all the other constraints to the model could also be relaxed, but this simple path seems the most promising to the authors.

The model described here succeeds in generating chemically sound interactions for equilibrium configurations and qualitative agreement on the different structural and dynamical features investigated in this work. However, the goal of this work is quite ambitious in its choice of chemical systems to be represented, and the simplicity of the model investigated here may prove to be a limitation on its ultimate quantitative success. In any case, a detailed comparison of dynamical results extracted from a well-defined model, such as the one derived here, and carefully measured experimental properties will inevitably lead to a deeper understanding of silicon–hydrogen surface chemistry.

References

- [1] H N Waltenburg, J T Yates, Jr, *Chem Rev* 95 (1995) 1589
- [2] F.H Stullinger, T A Weber, *Phys Rev B* 31 (1985) 5262
- [3] K Ding, H C Andersen, *Phys Rev B* 34 (1986) 6987.
- [4] F H Stullinger, T A Weber, *Phys Rev Lett* 62 (1989) 2144
- [5] T A Weber, F H Stullinger, *J. Chem Phys* 92 (1990) 6239
- [6] C J Wu, I V Ionova, E A Carter, *Phys Rev B* 49 (1994) 13488
- [7] M V R Murty, H A Atwater, *Phys Rev. B* 51 (1995) 4889
- [8] K P Huber, G. Herzberg, *Molecular Spectra and Molecular Structure 4 Constants of Diatomic Molecules*, Van Nostrand, New York, 1979
- [9] D L. Diedrich, J.B Anderson, *Science* 258 (1992) 786
- [10] D L. Diedrich, J B Anderson, *J Chem Phys* 100 (1994) 8089
- [11] M.W Chase, Jr, C A Davies, J.R. Downey, Jr, D J Frurip, R.A McDonald, A N Syverud, *J Phys Chem Ref Data* 14 (Suppl No 1) (1985)
- [12] Doncaster, Walsh, *Int J Chem. Kinet.* 13 (1981) 503
- [13] J Berkowitz, J P Green, H Cho, B Ruscic, *J Chem Phys* 86 (1987) 1235
- [14] *Gmelin Handbook of Inorganic and Organometallic Chemistry Silicon Supplement*, vol. B1, Springer, New York, 1982

- [15] K Raghavachari, personal communication
- [16] S Lias et al, *J Phys. Chem Ref Data* 17 (Suppl No 1) (1988)
- [17] J.B. Pedley, J Rylance, *Computer Analyzed Thermochemical Data Organic and Organometallic Compounds*, University of Sussex, 1977
- [18] F Shoji, K Kusumura, K Oura, *Surf Sci* 280 (1993) L247
- [19] W R Wampler, S.M Myers, D M Follstaedt, *Phys Rev B* 48 (1993) 4492
- [20] C J. Wu, E A Carter, *Chem Phys Lett* 185 (1991) 172
- [21] R Walsh, *Acc. Chem. Res.* 14 (1981) 246
- [22] J Boland, *Adv Phys* 42 (1993) 129
- [23] C.G Van de Walle, *Phys Rev B* 49 (1994) 4579
- [24] M D Allen, D J Tildesley, *Computer Simulation of Liquids*, Clarendon Press, Oxford, 1994
- [25] J T Law, *J Chem Phys* 30 (1959) 1568.
- [26] C.J Wu, I V Ionova, E A Carter, *Surf Sci* 295 (1993) 64
- [27] A Vittadini, A Selloni, M Casarin, *Surf. Sci* 289 (1993) L625
- [28] D J Doren, *Adv Chem Phys* XCV (1996) 1
- [29] M R Radeke, E A Carter, *Phys. Rev B* 54 (1996) 11803
- [30] Y J Chabal, K Raghavachari, *Phys Rev Lett* 53 (1984) 282
- [31] Y M Wu, J Baker, P Hamilton, R Nix, *Surf Sci* 295 (1993) 133
- [32] J Abrefah, D R Olander, *Surf Sci* 209 (1989) 291.
- [33] K W Kolasinski, W Nessler, K Bornscheuer, E J Hasselbrink, *J Chem Phys* 101 (1994) 7082